J Mater Sci (2010) 45:2938–2943
DOI 10.1007/s10853-010-4286-x

Biological synthesis of calcite crystals using *Scindapsus aureum* petioles

Long Chen · Yu Hua Shen · An Jian Xie · Qian Nan Cheng

Received: 8 October 2009 / Accepted: 30 January 2010 / Published online: 17 February 2010

Abstract We report a novel strategy for the biological synthesis of calcite crystals using the petioles of the plant *Scindapsus aureum*. The resultant calcite crystals were characterized by scanning electron microscopy, Fourier transform infrared (FT-IR) spectroscopy, X-ray powder diffractometry, and electron diffraction. The biomolecules of *S. aureum* petioles were confirmed by UV–Vis and FT-IR analysis. The results showed that the spherical or rhombohedral calcite crystals were obtained in the cells of *S. aureum* petioles. Biomimetic synthesis of calcium carbonate ($CaCO_3$) in aqueous solution containing extracts of *S. aureum* petioles was also performed to investigate the soluble biomolecules' influence on crystal growth of $CaCO_3$. It was found that twinborn spherical calcite crystals were formed, suggesting that the soluble biomolecules of *S. aureum* play a crucial role in directing the formation of calcite spherical particles. The possible mechanism of formation of $CaCO_3$ crystals using *S. aureum* is also discussed; the biomolecules of *S. aureum* may induce and control the nucleation and growth of $CaCO_3$ crystals.

Introduction

Biological systems are capable of generating inorganic materials such as calcium carbonate ($CaCO_3$), magnetic iron oxide, and amorphous silica with exquisite morphology at ambient temperature in water by the process of biomineralization [1]. Biomineralization occurs in many different species and tissues, including bone mineral, tooth enamel, and marine shells. Many of the mineralized tissues formed by organisms have structural and functional value, as well as advantageous mechanical properties. Mineral growth in biological systems is directed by assemblies of acidic proteins and/or glycoproteins and is often achieved by intercalation of some of the acidic macromolecules into the crystal lattice [2]. Biomimetic synthesis of $CaCO_3$ crystals has been studied in great detail due to their abundance in nature and also their important industrial applications in the paint, plastics, rubber, and paper industries. $CaCO_3$ often has three crystalline polymorphs, that is, vaterite, aragonite, and calcite, in order of increasing thermodynamic stability. Calcite is thermodynamically the most stable polymorph and often found in biominerals [3, 4]. In addition, three metastable forms—amorphous calcium carbonate, crystalline monohydrate $CaCO_3$, and hexahydrate $CaCO_3$—have also been reported recently [5].

A number of biomimetic templates or additives such as Langmuir monolayers [6, 7], dynamic liquid–liquid interfaces [8], self-assembled monolayers [9], lipid bilayer stacks [10], vesicles [11], functionalized micropatterned surfaces [12], and proteins extracted from $CaCO_3$-rich organisms [12] or synthetic molecules such as polymers [13] have been used for the synthesis of $CaCO_3$. We obtained calcite, vaterite, and aragonite with various morphologies using different amino acids, Mg^{2+} ions [14], as well as a new amino-carboxyl-chelating-agent, 4-BAPTA [15]. Very recently, we have also gained $CaCO_3$ hollow spheres and disks using bacteria [16], and obtained $CaCO_3$ crystals with complex forms using dextran beneath a dipalmitoylphosphatidylcholine monolayer [17].

L. Chen · Y. H. Shen (✉) · A. J. Xie · Q. N. Cheng
School of Chemistry and Chemical Engineering, Anhui University, Hefei 230039, People's Republic of China
e-mail: s_yuhua@163.com

L. Chen
Department of Chemistry, Huangshan University, Huangshan 245041, People's Republic of China
e-mail: chenlong200808@yahoo.com.cn

Elucidation of general biomineralization principles has followed from studies into the growth of minerals in biological organisms [2], and on biomacromolecules extracted from organisms [18]. Sastry and co-workers used fungi, actinomycetes, and germinating chickpea seeds to synthesize biogenic $CaCO_3$ crystals [19–22]. However, biomimetic synthesis of $CaCO_3$ crystals utilizing organisms and/or their extracts is rarely studied. In this article, we show that the biomolecules, especially the soluble biomolecules of *Scindapsus aureum* petioles, can direct the growth of hierarchical calcite spherical crystals, which are built up of small subunits. The possible biomineralization-associated formation mechanism of $CaCO_3$ crystals is also discussed. This report may represent an advance in developing this strategy to encompass other organisms and mineral compositions and underline the untapped potential of biological methods in expanding the scope of crystal engineering. Furthermore, it is very significant for biomineralization research and green synthesis of functional inorganic materials.

Experimental

Materials and instruments

Anhydrous calcium chloride ($CaCl_2$), ammonium carbonate ($(NH_4)_2CO_3$), and ethanol were purchased from Shanghai Reagent Plant (Shanghai, China), and were analytically pure. They were used without further purification. The plant *S. aureum* (Fig. 1) was purchased from a local farmer. Double-distilled water was used in all experiments.

The samples were characterized by Fourier transform infrared (FT-IR) spectroscopy (Nicolet 870, USA) using KBr pellets over the wave number range of 400–4000 cm^{-1} with a resolution of 4 cm^{-1} and X-ray diffractometer (DX-2000, Japan) using CuKα radiation at a scan rate of 0.06° $2\theta \cdot S^{-1}$. The morphologies of the samples were observed by scanning electron microscopy (SEM) (Hitachi X-650, Japan) with an accelerating voltage of 20 kV. Electron diffraction (ED) of them was carried out on a JEM model 100SX electron microscope instrument (Japan Electron Co.) operated at an accelerating voltage at 200 kV. A UV–Vis double-beam spectrophotometer (Beijing Purkinje General Instrument Co., Ltd, China) was also used.

Fig. 1 The plant *S. aureum* used in our experiments

In vivo synthesis of $CaCO_3$ in the cells of *S. aureum* petioles

A petiole of the fresh-gained *S. aureum* was cut open with a knife, and the vertical sections of them were examined by SEM for observing its cells before cultivation. A small amount of *S. aureum* petioles were crushed, and then mixed with solid KBr, dried, and examined by FT-IR for characterizing their chemical composition. Then, the *S. aureum* was watered every morning and every evening using 50 mL 0.01 M $CaCl_2$ aqueous solution each time. After watering, the *S. aureum* was exposed to sunlight for 1–2 h by placing near the open window of our lab. After 20 days of cultivation (plant is shown in Fig. 1), a petiole of the plant was cut open and the vertical sections of it were examined by SEM for observing the morphology of $CaCO_3$ grown in it. Crystal phase of the $CaCO_3$ particles was determined by ED.

In vitro synthesis of $CaCO_3$ using the extracts of *S. aureum* petioles

In order to investigate the influence of *S. aureum* petioles' soluble biomolecules on crystal growth of $CaCO_3$, 11.5 g of *S. aureum* petioles were washed carefully, and then immersed in 3% H_2O_2 solution for 5 min. After that, the petioles were crushed to extract juice, and the juice was mixed with proper amount of double-distilled water, obtaining 50 mL of *S. aureum* petiole extract aqueous solution. This solution was first examined by UV–Vis spectroscopy for understanding the soluble biomolecules of *S. aureum* petioles. Then, the solution was mixed with the same volume of 0.1 M $CaCl_2$ or 0.01 M $CaCl_2$, completely, obtaining 100 mL of mixed solution containing *S. aureum* extracts and 0.05 M or 0.005 M $CaCl_2$. Two glass beakers containing *S. aureum* extracts and 0.05 M or 0.005 M $CaCl_2$ solutions were covered with PVC film, each of which was punched with three needle holes and placed in a larger desiccator. A 50-mL glass beaker containing 2.0 g of solid crushed ammonium carbonate covered with PVC film and punched with three needle holes was placed at the bottom of the desiccator. This desiccator

was closed and maintained at a temperature of 22–24 °C for 24 h.

The white precipitates produced in the reaction solution containing *S. aureum* petiole extracts were separated by centrifugation (4,000 rpm), washed three times with double-distilled water and ethanol, and then vacuum dried for further determination.

The size and morphology of the precipitates were examined by SEM, whereas their crystal phases were determined by FT-IR spectroscopy or X-ray powder diffractometry (XRD).

Results and discussion

Figure 2 presents SEM images of *S. aureum* petiole's vertical section before and after it was cultivated by using 0.01 M $CaCl_2$ solution. From Fig. 2a, it can be seen that no obvious inorganic crystals appeared in the cells of *S. aureum* petiole before it was cultivated. On the other hand, many inorganic particles are produced in the cells after the plant was cultivated by using 0.01 M $CaCl_2$ solution for 20 days (Fig. 2b–d). From the magnified images (Fig. 2c, d), it can be seen that the particles obtained have two kinds of morphologies, spherical and rhombohedral. The mean diameter of the spheres is about 2 μm, and the average size of the rhombohedrons is 2.5 × 1 × 0.5 μm^3. The electron diffraction patterns (insets in Fig. 2d) demonstrate that the two kinds of particles are both calcite crystals. The above-mentioned results suggest that $CaCO_3$ can be precipitated in its most stable form in the cells of *S. aureum* petiole, and the biomolecules of the plant petiole may direct the morphology of the calcite crystals obtained.

Figure 3 shows SEM images of $CaCO_3$ particles obtained in $CaCl_2$ aqueous solution containing extracts of *S. aureum* petioles. When the concentration of $CaCl_2$ is 0.005 M, the $CaCO_3$ particles obtained are twinborn spheres (Fig. 3a). The average diameter of the spheres is about 9 μm. From the enlarged image (Fig. 3b), it is evident that surface of the sphere is very coarse. Careful observation reveals that the big spheres are constructed from small nanoparticles. The crystal phase of the $CaCO_3$ is confirmed by FT-IR spectrum. Figure 4 shows the related FT-IR spectrum of $CaCO_3$ particles obtained. The peaks located at 712 and 872 cm^{-1} correspond to the in-plane bending and out-of-plane bending modes of CO_3^{2-}, respectively, and they are also characteristic of calcite. The peak at 1425 cm^{-1} is assigned to the asymmetric C–O stretching vibration and it is also characteristic of $CaCO_3$. A weak peak at 2514 cm^{-1} is characteristic of calcite in accordance with the infrared spectra of calcite in NIST Chemistry Webbook [17], further confirming the products are calcite.

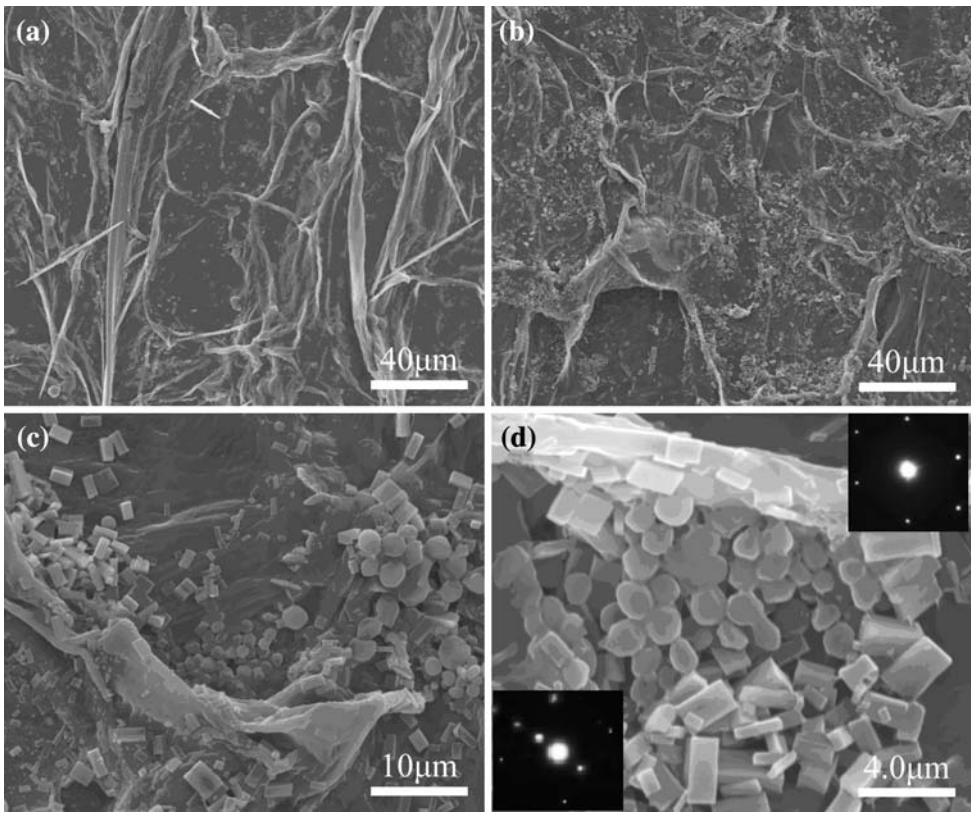

Fig. 2 SEM images of vertical section of *S. aureum* petiole before (**a**) and after (**b–d**) it cultivated by using 0.01 M $CaCl_2$ solution. **c** and **d** are magnifications of (**b**). The *insets* in (**d**) are ED pattern of the $CaCO_3$ particles (*top right corner* spherical particles, *bottom left corner* rhombohedral particles)

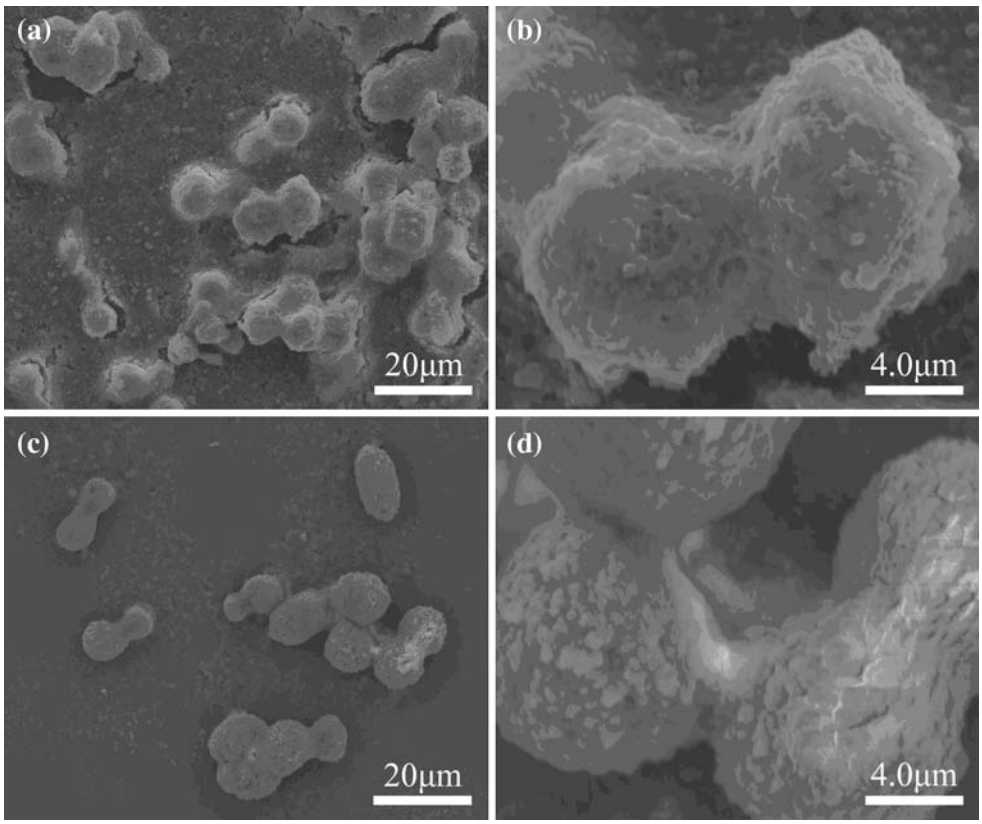

Fig. 3 SEM images of $CaCO_3$ particles obtained in different concentration of $CaCl_2$ aqueous solution containing extracts of *S. aureum* petiole (**a**, **b**: $[CaCl_2] = 0.005$ M; **c**, **d**: $[CaCl_2] = 0.05$ M). **b** and **d** are magnifications of **a** and **c**, respectively

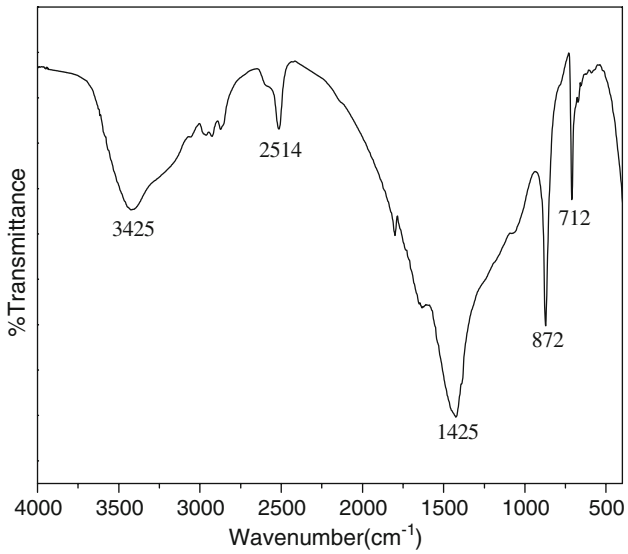

Fig. 4 FT-IR spectrum of $CaCO_3$ particles obtained in 0.005 M $CaCl_2$ aqueous solution containing extracts of *S. aureum* petioles

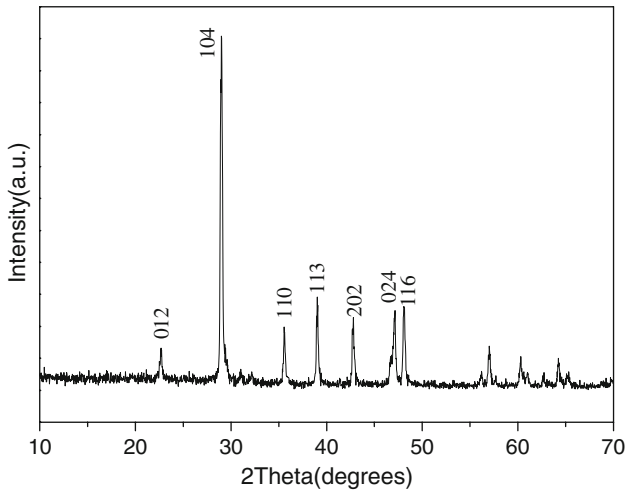

Fig. 5 XRD pattern of $CaCO_3$ particles obtained in 0.05 M $CaCl_2$ aqueous solution containing extracts of *S. aureum* petioles

When the concentration of $CaCl_2$ in the solution containing *S. aureum* extracts is increased to 0.05 M, twinborn spherical particles with average diameter of about 9 μm are produced (Fig. 3c, d). In other words, the products have no obvious change in morphology and size as the concentration of $CaCl_2$ is increased. Crystal phase of the products is determined by XRD. Figure 5 shows that the XRD pattern of the $CaCO_3$ crystals obtained displays the following diffraction peaks (2θ [°]): 23.01, 29.34, 35.92, 39.38, 43.12, 47.30, and 48.50, which can be correlated to the *hkl* indices (012), (104), (110), (113), (202), (024), and (116), respectively, of calcite (JCPDS card number: 72-1652). This indicates that the products are also calcite.

The results suggest that the soluble biomolecules of *S. aureum* can only influence the nucleation, crystal growth, and morphology of calcite. On the other hand, they are not capable of stabilizing the unstable phase of $CaCO_3$ such as vaterite. According to [23], the growth mechanism of $CaCO_3$ spherical crystals with complex surface structures composed of small subunits may be as follows. At first, unstable vaterite nanospheres form, which subsequently aggregate to spherical particles. Later, transformation to calcite beginning on the surface leads to the formation of calcite nanoparticles on the particle surface. These nanoparticles then grow at the expense of the dissolving vaterite particles by Ostwald ripening.

Petiole of *S. aureum* is composed of many biomolecules. We studied its chemical composition by means of UV–Vis and FT-IR spectroscopy. UV–Vis spectrum of the *S. aureum* petiole extracts solution is shown in Fig. 6a. The peak at 210 nm is assigned to the strong absorption of peptide bonds of protein in the extract, which rose owing to the stemming from n–π^* transition of C=O group. The absorption at 280 nm is belonged to the π–π^* transition of

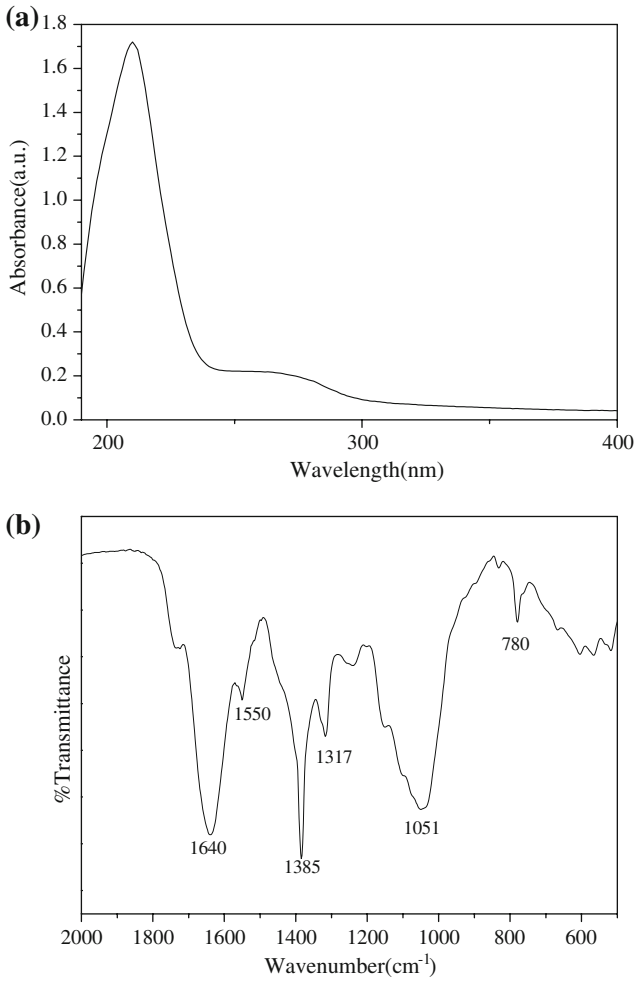

Fig. 6 **a** UV–Vis and **b** FT-IR spectra of *S. aureum* petioles

tyrosine, tryptophan, or phenylalanine residues of proteins. Therefore, it can be concluded that *S. aureum* petiole contains proteins. Figure 6b shows FT-IR spectrum of *S. aureum* petioles. The absorption bands at 1640 and 1543 cm^{-1} are assigned to amide I($\nu_{C=O}$) and II(δ_{N-H}) of protein, respectively, further confirming that they contain protein(s). The peaks located at 1385, 1317, and 1051 cm^{-1} may correspond to the chlorophyll macrocyclic skeleton vibration.

In biological systems, it is widely accepted that highly anionic, soluble biomacromolecules such as acidic proteins, glycoproteins, and polysaccharides play an important role in biomineralization, and act as nucleators, growth modifiers, and anchoring units in mineral formation [2]. It is evident from above findings that *S. aureum* petioles contain certain amount of biomolecules in the form of proteins. It can be speculated that the biomolecules such as proteins play a crucial role in defining the morphology of $CaCO_3$. In our opinion, the growth of the crystals may proceed in the following manner. In the first step, the Ca^{2+} ions in the cells or solution reacts with the biomolecules such as proteins of *S. aureum* leading to the formation of stable aggregates. The entrapped Ca^{2+} ions then react with CO_2 produced by the cells of *S. aureum* petiole or decomposition of $(NH_4)_2CO_3$ in situ, thereby forming $CaCO_3$ crystals. During the growth process of $CaCO_3$ crystals, the biomolecules may adsorb onto certain facets of the crystals and define the morphology of $CaCO_3$.

According to the nucleation theory [24], the nucleation rate J depends on the level of solution supersaturation S, the crystal-medium interfacial energy γ, and the pre-exponential factor A (the value of which is determined by the rate of attachment of growth units to the aggregating nuclei) by the relation

$$J = A \exp\left(-\frac{16\pi\gamma^3\Omega^2}{3k^3T^3\ln^2 S}\right) \quad (1)$$

where k is the Boltzmann constant, T is the temperature, and Ω is the molecular volume. The nucleation rate J of $CaCO_3$ can increase with the increase in the pre-exponential factor A, reduction in the interfacial energy γ, and/or increase in the supersaturation S. The negatively charged groups, such as $-COO^-$, of the biomolecules such as proteins can first bind Ca^{2+} strongly to provide nucleation sites. Then, the enriched Ca^{2+} ions may attract anions CO_3^{2-} thereby leading to an increase in the rate of attachment of growth units to the aggregating nuclei A and supersaturation S, and a decrease in the interfacial energy γ for the formation of $CaCO_3$ nuclei by heterogeneous nucleation. Consequently, the nucleation rate of $CaCO_3$ crystals is accelerated by the inducement of *S. aureum* petiole biomolecules.

Conclusions

Biological synthesis of calcite crystals using *S. aureum* petioles was studied. The spherical or rhombohedral calcite crystals were obtained in the cells of *S. aureum* petioles. Biomimetic synthesis of $CaCO_3$ in aqueous solution containing extracts of *S. aureum* petioles was also performed, suggesting that twinborn spherical calcite crystals were formed. The possible formation mechanism of the $CaCO_3$ crystals by using *S. aureum* petioles is discussed, showing that the biomolecules of *S. aureum* may induce and control the nucleation and growth of $CaCO_3$ crystals.

Acknowledgements This work was supported by the National Science Foundation of China (20671001, 20871001, 20731001), the Important Project of Anhui Provincial Education Department (ZD2007004-1), the Research Foundation for the Doctoral Program of Higher Education of China (20070357002), the Specific Project for Talents of Science and Technology of Universities of Anhui Province (2005hbz03), the Foundation of Key Laboratory of Environment-friendly Polymer Materials and Functional Material of Inorganic Chemistry of Anhui Province, and the Project of Huangshan University (2008xkjq018).

References

1. Sarikaya M (1999) Proc Natl Acad Sci USA 96:14183
2. Berman A, Hanson J, Leiserowitz L, Koetzle TF, Weiner S, Addadi L (1993) Science 259:776
3. Lakshminarayanan R, Kini RM, Valiyaveettil S (2002) Proc Natl Acad Sci USA 99:5155
4. Kato T, Sugawara A, Hosoda N (2002) Adv Mater 14:869
5. Xu AW, Yu Q, Dong WF, Antonietti M, Cölfen H (2005) Adv Mater 17:2217
6. Loste E, Marti ED, Zarbakhsh A, Meldrum FC (2003) Langmuir 19:2830
7. Xue ZH, Dai SX, Hu BB, Du ZL (2009) Mater Sci Eng C 29:1998
8. Rautaray D, Banpurkar A, Sainkar SR, Limaye AV, Pavaskar NR, Ogale SB, Sastry M (2003) Adv Mater 15:1273
9. Kuther J, Nelles G, Seshadri R, Schaub M, Butt HJ, Tremel W (1998) Chem Eur J 4:1834
10. Damle C, Kumar A, Bhagwat M, Sainkar SR, Sastry M (2002) Langmuir 18:6075
11. Walsh D, Mann S (1995) Nature 377:320
12. Aizenberg J, Muller DA, Grazul JL, Hamman DR (2003) Science 299:1205
13. Qi L, Li J, Ma J (2002) Adv Mater 14:300
14. Xie AJ, Shen YH, Zhang CY, Yuan ZW, Zhu XM, Yang YM (2005) J Cryst Growth 285:436
15. Xie AJ, Yuan ZW, Shen YH (2005) J Cryst Growth 276:265
16. Chen L, Shen YH, Xie AJ, Huang B, Jia R, Guo RY, Tang WZ (2009) Cryst Growth Des 9:743
17. Huang FZ, Shen YH, Xie AJ, Yu SH, Chen L, Zhang BC, Chang WG (2009) Cryst Growth Des 9:722
18. Falini G, Albeck S, Weiner S, Addadi L (1996) Science 271:67
19. Rautaray D, Ahmad A, Sastry M (2003) J Am Chem Soc 125:14656
20. Rautaray D, Ahmad A, Sastry M (2004) J Mater Chem 14:2333
21. Ahmad A, Rautaray D, Sastry M (2004) Adv Funct Mater 14:1075
22. Rautaray D, Sanyal A, Bharde A, Ahmad A, Sastry M (2005) Cryst Growth Des 5:399
23. Yu SH, Cölfen H, Antonietti M (2003) J Phys Chem B 107:7396
24. Chen L, Xie AJ, Jia R, Shen YH, Tang WZ, Li CH (2007) Cryst Res Technol 42:881